(2)

TECHNICAL REPORT BRL-TR-3200

BRL

HIGH STRAIN RATE RESPONSE OF GUN PROPELLANT USING THE HOPKINSON SPLIT BAR

ROBERT J. LIEB

FEBRUARY 1991

U.S. ARMY LABORATORY COMMAND

BALLISTIC RESEARCH LABORATORY
ABERDEEN PROVING GROUND, MARYLAND

NOTICES

Destroy this report when it is no longer needed. DO NOT return it to the originator.

Additional copies of this report may be obtained from the National Technical Information Service, U.S. Department of Commerce, 5285 Port Royal Road, Springfield, VA 22161.

The findings of this report are not to be construed as an official Department of the Army position, unless so designated by other authorized documents.

The use of trade names or manufacturers' names in this report does not constitute indorsement of any commercial product.

UNCLASSIFIED

REPORT DOCUMENTATION PAGE

Form Approved
OMB No. 0704-0188

1. AGENCY USE ONLY (Leave blank)	2. REPORT DATE	3. REPORT TYPE AND DATES COVERED
	February 1991	Final, Oct 88 - Feb 89

4. TITLE AND SUBTITLE

High Strain Rate Response of Gun Propellant Using the Hopkinson Split Bar

5. FUNDING NUMBERS

PR: 1L161102AH43

6. AUTHOR(S)

Robert J. Lieb

7. PERFORMING ORGANIZATION NAME(S) AND ADDRESS(ES)

US Army Ballistic Research Laboratory
ATTN: SLCBR-IB-P
Aberdeen Proving Ground, MD 21005-5066

8. PERFORMING ORGANIZATION REPORT NUMBER

9. SPONSORING / MONITORING AGENCY NAME(S) AND ADDRESS(ES)

US Army Ballistic Research Laboratory
ATTN: SLCBR-DD-T
Aberdeen Proving Ground, MD 21005-5066

10. SPONSORING / MONITORING AGENCY REPORT NUMBER

BRL-TR-3200

11. SUPPLEMENTARY NOTES

12a. DISTRIBUTION / AVAILABILITY STATEMENT

Approved for Public Release; Distribution Unlimited

12b. DISTRIBUTION CODE

13. ABSTRACT *(Maximum 200 words)*

The Hopkinson Split Bar has been shown to be a useful tool to investigate the high rate response of gun propellant. The mechanical responses of M30, JA2, and XM39 propellants were measured at strain rates ranging from 1000/s to over 10,000/s. Results reported here show that yield stress and modulus generally increase, and that yield strain decreases with increasing strain rate. Some effects of porosity and specimen size are also reported.

14. SUBJECT TERMS

Mechanical Properties, Propellants, High Rate, M30, JA2, XM39, Compressive Testing, Hopkinson Split Bar

15. NUMBER OF PAGES

29

16. PRICE CODE

17. SECURITY CLASSIFICATION OF REPORT	18. SECURITY CLASSIFICATION OF THIS PAGE	19. SECURITY CLASSIFICATION OF ABSTRACT	20. LIMITATION OF ABSTRACT
UNCLASSIFIED	UNCLASSIFIED	UNCLASSIFIED	

Intentionally Left Blank

TABLE OF CONTENTS

A-1

Intentionally Left Blank

LIST OF FIGURES

LIST OF TABLES

I. INTRODUCTION

The mechanical response of gun propellant to high rate deformation plays a critical role in the performance of guns and in the violence of the response of the propellant to vulnerability threats. However, unlike engineering materials, which have most of their critical characterizations performed within a range of state from stress-free up to conditions of failure, propellant performance is most affected by mechanical response only after failure has occurred. Indeed, the changes in propellant dimensions, under ideal firing conditions where no failure occurs, have been shown, using ballistic code analysis, to have almost no effect on gun performance[1]. Propellant performance within an established charge depends on the rate of generation of gases through combustion (mass generation rate). This mass generation rate of the propellant depends on its burning rate, density, and the total surface area undergoing combustion. This relationship can be expressed by the following:

$$dm/dt = \rho r A \qquad (1)$$

where dm/dt is the mass generation rate, ρ is the mass density, r is the pressure dependent burning rate, and A is the exposed surface area. The variable critically influenced by the mechanical response is A. The purpose of this study, then, is to help characterize the propellant susceptibility to fracture which can be evaluated by measuring changes in the propellant mechanical response. If the propellant is properly characterized, this susceptibility can be compared to acceptable performers or used to point out response characteristics that need to be changed to enhance performance.

Until propellant failure conditions exist within the gun, A is a well behaved parameter. Unprogrammed generation of surface area can come from several sources. If individual grains are projected against interior surfaces, such as cartridge case walls, the projectile base, or protruding projectile fins, single grain impact results. The amount of fracture generated surface area will depend on factors such as the impact velocity, orientation, geometry and temperature of the grain. Grain-grain interaction is also possible and has been described as an intergranular stress wave propagating through the bed. If this stress state exceeds critical limits, fracture surface area will be generated. A third failure mechanism results when the pressure differences between the gun chamber and the perforation within the grain exceed critical values. This results in the grain or stick bursting or collapsing, and unprogrammed surface area being added during the combustion process.

Until recently, only low rate (static to strain rates of 1/s), low pressure (atmospheric) mechanical response measurements were made on these materials. Since most propellants are polymeric systems that may or may not be filled, the response is sensitive to the rate of testing. Strain rates experienced within the ballistic environment are thought to range from 10 to 500/s and may extend to as high as 10,000/s under certain conditions. Intermediate rate (100 to 300/s) testing has been performed routinely at the Ballistic Research Laboratory for the past five years. Much has been learned about the fracture response of propellants at these rates, and these findings have been reported in the literature[2, 3, 4, 5]. Response measurements at rates greater than these have been performed at Lawrence Livermore National Laboratory by Costantino and Ornellas[6, 7]. The LLNL results are provided in this report for comparison.

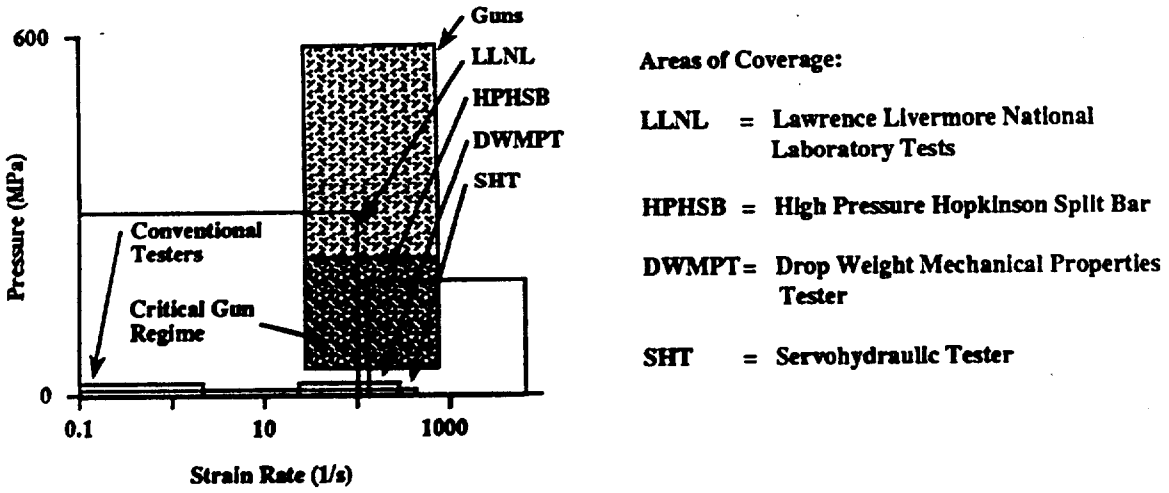

Figure 1. Comparison of the Pressure-Strain Rate Regime of Ballistic Interest and the Capability of Measurement Devices

A comparison between the pressure-strain rate range of ballistic interest and the range over which testing is possible is illustrated in Figure 1. It can be seen that some encroachments into the operating regime of the gun (shaded region) have been made. The darker shaded region represents conditions early in the ballistic cycle, and is considered critical because any mechanical failure that produces significant increases in mass generation will have the potential of generating severe adverse effects on the remainder of the ballistic cycle. A large section of this critical gun regime can be investigated using a High Pressure Hopkinson Split Bar (HPHSB). This served as an impetus for the development of such a device.

The Hopkinson Split Bar (HSB) has long been a useful tool to explore the high rate (500 to 10,000/s) mechanical response of materials. This technique has been successfully applied to a variety of materials including gun propellants for the evaluation of mechanical and fracture response at very high strain rates. The HSB was constructed at BRL to determine the propellant response at high strain rates, and as the first effort in the construction of a high pressure variation to explore the critical portion of the gun pressure-rate regime, indicated in Figure 1. A description of the HSB and its operation will be outlined. Earlier results from tests conducted during the construction of this device were reported in Reference 8. The results of the most recent experiments performed on M30, JA2 and XM39 propellants are presented here.

II. THEORY OF OPERATION

There are many sources that provide a detailed presentation of the theory of operation of the HSB[9, 10, 11, 13] and the reader is referred to these for more specific information. However, a general description is provided here to facilitate understanding of the bar for those unfamiliar with the device.

The HSB provides a means by which high rate deformation can be applied to a specimen, and the mechanical response of the material can be measured. The device consists of a projectile launcher, a striker projectile and a pair of bars, the input bar and output bar, as illustrated in Figure 2. In

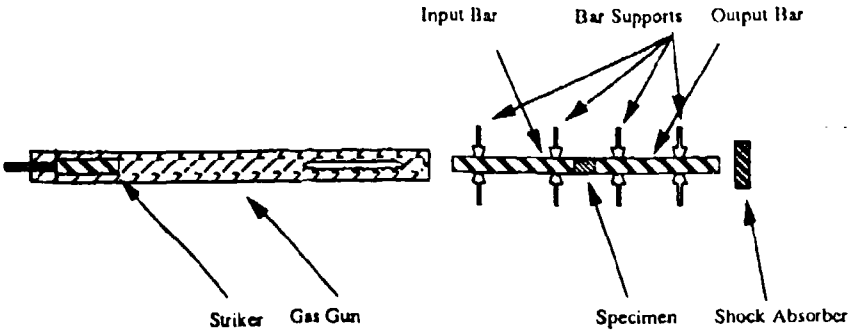

Figure 2. Schematic Diagram of the Gas Gun and the Hopkinson Split Bar

operation, a stress pulse passes through the input bar and deforms the specimen which is located between bars. As deformation occurs the specimen stress response to the deformation is transmitted to and proceeds along the output bar. The reflected stress wave from the input bar-specimen interface characterizes the interaction between the this bar and specimen, and determines the specimen deformation. The output bar carries the stress pulse corresponding to this deformation and if the assumption of mechanical equilibrium of the specimen is made, then the specimen stress and strain can be extracted from these two pulses.

This process is illustrated in Figure 3. The striker impacts the input bar which initiates a stress pulse in that bar. The duration of the pulse is dependent on the length of the striker. The magnitude of the stress pulse is determined by the impact velocity of the striker and the mechanical impedance match between the striker and input bar. To facilitate a good mechanical impedance match, the striker and input bar are often made of the same material and have similar diameters. As this pulse passes the strain gages, mounted on opposite sides of the input bar, the first strain pulse is measured. In this example the stress begins to pass the gage at about 0.05 ms. At 0.15 ms the pulse begins to deform the specimen and a reflected tensile wave starts back toward the input bar gage, while a transmitted compressive pulse begins in the output bar. At about 0.3 ms the reflected and transmitted pulses begin to be detected by their respective gages. Finally at about 0.4 ms the end of these pulses passes the gages and experiment is over. However, reflection will continue to occur at the ends of each bar. Note that the length of the striker is limited by the requirement that the initial and reflected pulses must not be interfering at the strain gage location. Thus the maximum length for a striker made of the same material as the bar is one-half the input bar length.

As mentioned above, the strain in the bars was measured using two active gages. These gages were located on opposite sides of a full bridge circuit to cancel any bending that may have been induced by an off-axis striker impact. Figure 4 shows a schematic diagram of this circuit. The relationships below were used to calculate the specimen response. The reflected input bar strain, ε_r, was calculated using the following equation[12]:

$$\varepsilon_r = \left(\frac{2}{F}\right)\left(\frac{V_0}{V}\right)\left(\frac{1}{1-\frac{V_0}{V}}\right) \qquad (2)$$

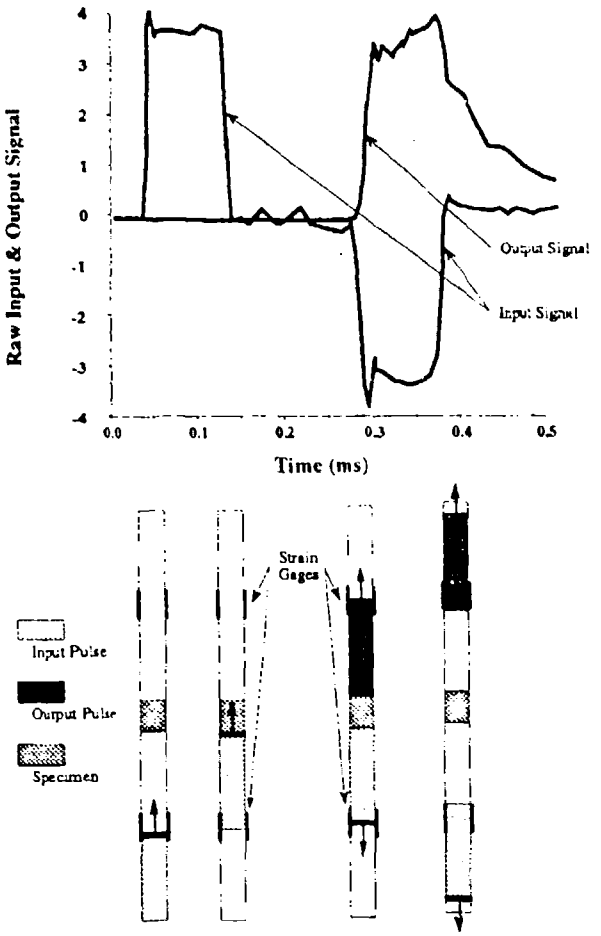

Figure 3. The Raw Signal Output from the HSB and the Corresponding Stress Pulses in the Bars

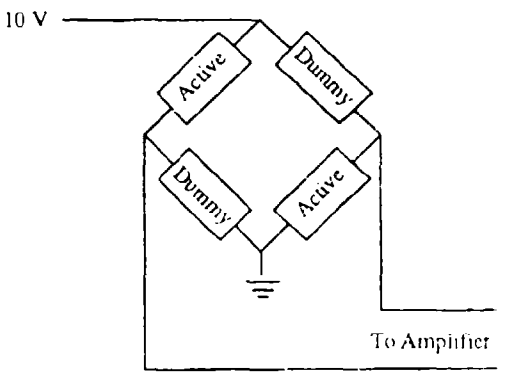

Figure 4. Schematic Diagram of the Strain Gage Bridge Circuit Used on the Input and Output Bars

where F is the gage factor, V_0 in the signal voltage, and V is the bridge excitation voltage. The third term on the right hand side of the equation is a nonlinear correction factor for the circuit. The specimen strain, ε_s, at time t is given by the following relationship[13]:

$$\varepsilon_s = -\frac{2C_0}{L}\int_0^t \varepsilon_r \, dt \qquad (3)$$

where C_0 is the sound speed within the input bar, and L is the length of the specimen. The stress within the specimen, σ_s is determined by:

$$\sigma_s = \left(\frac{A}{A_s}\right) E \, \varepsilon_T \qquad (4)$$

where A is the cross sectional area of the output bar, A_s is the cross sectional area of the specimen, E is the modulus of the output bar, and ε_T is the strain transmitted to the output bar, which was calculated from an equation similar to Equation 2. This set of equations was used to determine the stress and strain response of the specimen to the high rate deformation.

III. APPARATUS AND PROCEDURE

A. The Apparatus

The Hopkinson Split Bar used in these tests, illustrated in Figure 2, consists of elastic input and output bars of equal length (120.0 cm) and diameter (1.25 cm). The striker (23.0 cm in length) was accelerated to impact velocities by means of a gas gun. The bars and striker were made of aluminum to provide a good impedance match between specimen and the bars. The 1000-ohm strain gages were mounted on opposite sides of each bar and provided the input to conditioning amplifiers. The two-channel output from the conditioning amplifiers was recorded using two 2.5 MHz amplifiers.

B. Specimen Preparation and Conditioning

Right circular cylinder specimens of M30, JA2, and XM39 gun propellant were prepared by cutting either propellant grains (7-multiperforated) or solid rods with a diamond saw so that each end was flat to within 10 μm, parallel to the opposite end to within 0.25°, and perpendicular to the axis of the cylinder to within 0.5°. The specimens had a length to diameter ratio of 1 ± 0.05, except in several cases where higher strain rates were desired. In those cases the ratio ranged from about 0.6 to 0.2. All tests were conducted at ambient temperatures (19-24°C) and pressures (0.1 MPa). The composition of these propellants is given in Table 1.

C. The Procedure

Preparation of the Hopkinson Split Bar is necessary before measurements can be made. The bar must be aligned so that the striker, input and output bars are coaxial. The ends of bars must be mated to ensure that pulse asymmetries generated by the impact are kept to a minimum. A mismatch between any two components will produce signal noise. Ideally, the input pulse should be a square wave. The less square the wave is the less aligned or mated the bars are.

Calibration shots were made with no sample present to check striker-bar alignment, and the transmittal of the pulse across the input-output bar interface. If all elements were correctly aligned, a square pulse would be generated and transmitted to the output bar with no reflection at thebar interface. The pulse rise and fall should be rapid and clean with no overshoot or rounded edge. When the calibration shots were found to be acceptable, specimens were introduced into the system.

The ends of the specimen were coated with a very thin layer of molybdenum disulfide paste to reduce shear friction between the bar and specimen. The specimen was then placed between the input and output bars so that the axis of the specimen was aligned with the bar axes. A striker velocity was selected so that strain rates on the order of 1000/s were achieved, except in the thin sample cases where rates of about 10,000/s were desired. The gas gun reservoir was charged with nitrogen and released remotely to initiate striker acceleration.

Table 1. Percent Composition of JA2, M30, and XM39 Gun Propellants

Component	JA2	M30	Component	XM39
Nitrocellulose	59	28	RDX (Ground)	76.0
NC Nitration Level	13.0	12.6	Celluiose Acetate Butyrate	12.0
Nitroglycerin	15	22	Acetyl Triethyl Citrate	7.6
Nitroguanidine	0	48	Nitrocellulose	4.0
Ethyl Centralite	0	2	NC Nitration Level	12.6
Diethylene Glycol Dinitrate	25	0	Ethyl Centralite	0.4
Akardit II	1	0		

Table 2. Key to the Parameters Reported in Figures 5 Through 8.

L	=	Specimen Length	3S	=	Stress at 3 % Strain
D	=	Specimen Diameter	5S	=	Stress at 5 % Strain
XA	=	Specimen X-Sec. Area	SY	=	Strain at Yield Stress
T	=	Specimen Temperature	SR	=	Strain Rate
P	=	Specimen Confining Pressure	E	=	Compressive Modulus
			EF	=	Failure Modulus
YS	=	Yield Stress	T'	=	Toughness at Yield

The data acquisition rate was 400 ns per point (2.5 MHz), which provided a sufficient number of points for analysis. Since the stress and strain information is recorded independently and away from the site of the specimen, the onset of stress and strain must be matched or shifted in time to agree. This was done during the data reduction in a manner such that the onset of the calculated stress curve was shifted to match the onset of the calculated strain curve. Scanning Electron Microscopy (SEM) was performed on tested specimens to explain some response features, which is discussed below.

Seven-multiperforated specimens of M30, JA2, and XM39 propellant were tested as well as solid stick M30. Specimens were prepared with length to diameter ratios of 1 and thinner specimens ($0.6 > L/D > 0.2$) of each propellant were prepared to explore higher rate deformation response. Five specimens were tested under each condition.

IV. RESULTS AND DISCUSSION

Typical results for specimens with a length to diameter ratio of 1 are given in Figures 5 through 7. Figure 5 also indicates the meaning of some of the parameters within the figures. These parameters are described more fully in Reference 2. Figures 6 and 7 include curves from earlier, lower rate testing for comparison. A key to the symbols is given in Table 2.

From these curves three different responses can be seen. M30 was very stiff before yielding at a stress significantly below expected, and then became much softer as deformation continued. This low yielding stress was unexpected because in lower rate tests using a Drop Weight Mechanical Properties Tester (DWMPT)[2] higher yield stresses were observed. Subsequent testing was performed on multiperforated specimens and will be discussed below. JA2 acted in a manner similar to lower rate tests. It deformed in an apparent elastic fashion until yield and then continued to undergo plastic deformation at that yield stress. The yield stress and modulus were higher than at lower rates, as expected, and the strain at yield was lower, indicating a trend toward more brittle response than at lower rates. XM39 also responded like it had previously in lower rate DWMPT tests. The yield stresses were about the same as those of the lower rate tests, but the modulus increased and the strain at yield decreased, indicating a more brittle response in these tests. After yielding the stress decreased with continued deformation, indicating a loss of strength due to fracture. Table 3 lists the average values obtained from these tests and the corresponding values obtained earlier from DWMPT tests.

Hopkinson
Split-Bar Test

ID = 1.072

L = 12.50 mm
D = 12.50 mm
XA = 122.7 mm
T = 25.00 C
P = .1000 MPa

YS = 58.19 MPa
3S = 80.37 MPa
5S = 93.36 MPa

SY = 0.615 Pct
SR = 1087 1/s

E = 12.28 GPa
EF = -.848 MPa
T' = 0.234 MPa

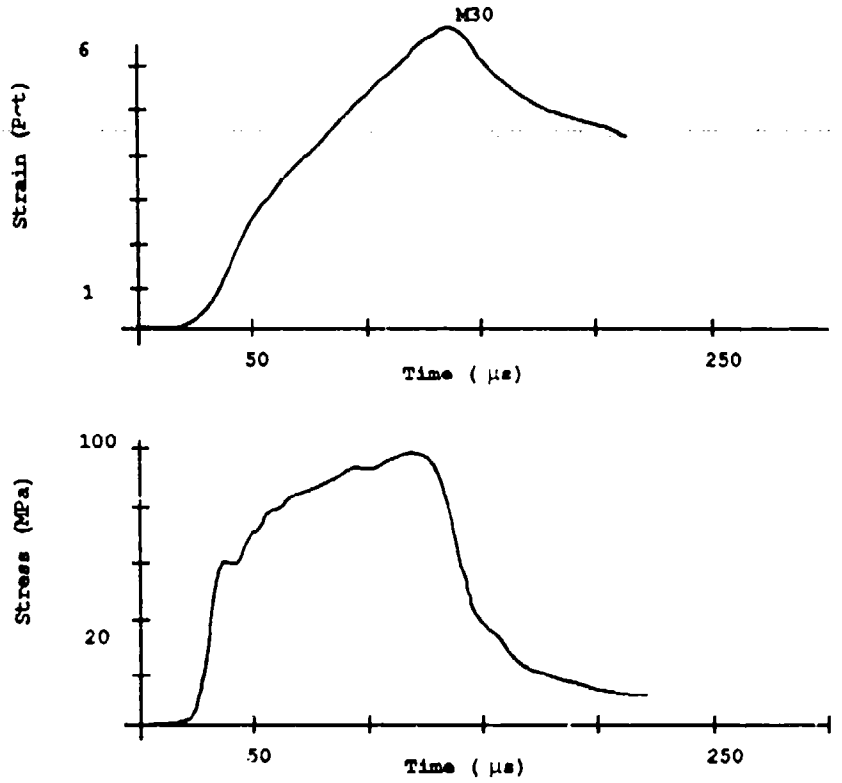

Figure 5a. Stress and Strain vs Time

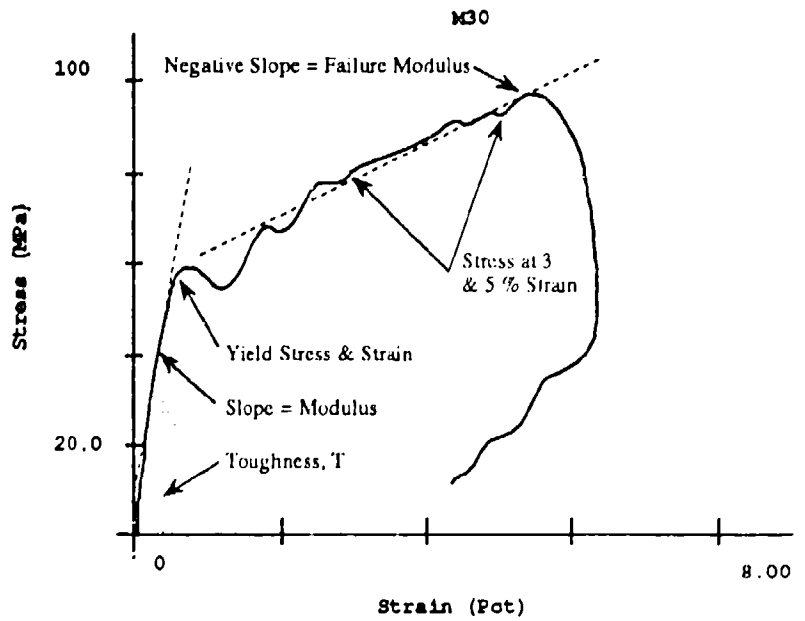

Figure 5b. Stress vs Strain

Figure 5. High Rate Response Curves for M30 Solid Stick Propellant

Hopkinson
Split-Bar Test

ID = 1.096

L = 8.920 mm
D = 8.760 mm
XA = 59.00 mm
T = 25.00 C
P = .1000 MPa

YS = 28.86 MPa
3S = 26.26 MPa
5S = 27.74 MPa

SY = 1.860 Pct
SR = 2023 1/s

E = 1.962 GPa
EF = -.054 MPa
T' = 0.340 MPa

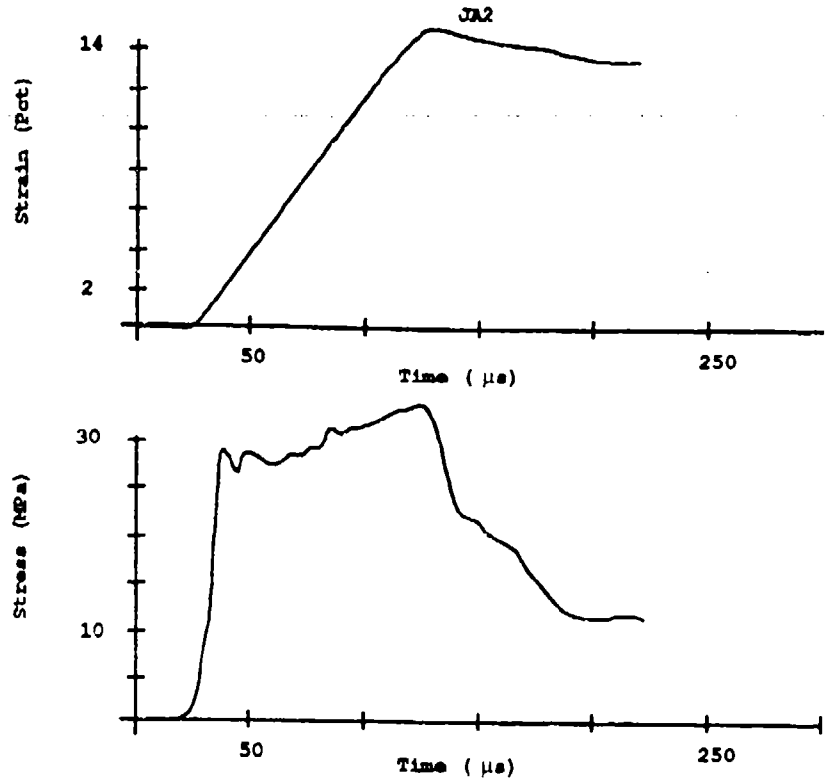

Figure 6a. Stress and Strain vs Time

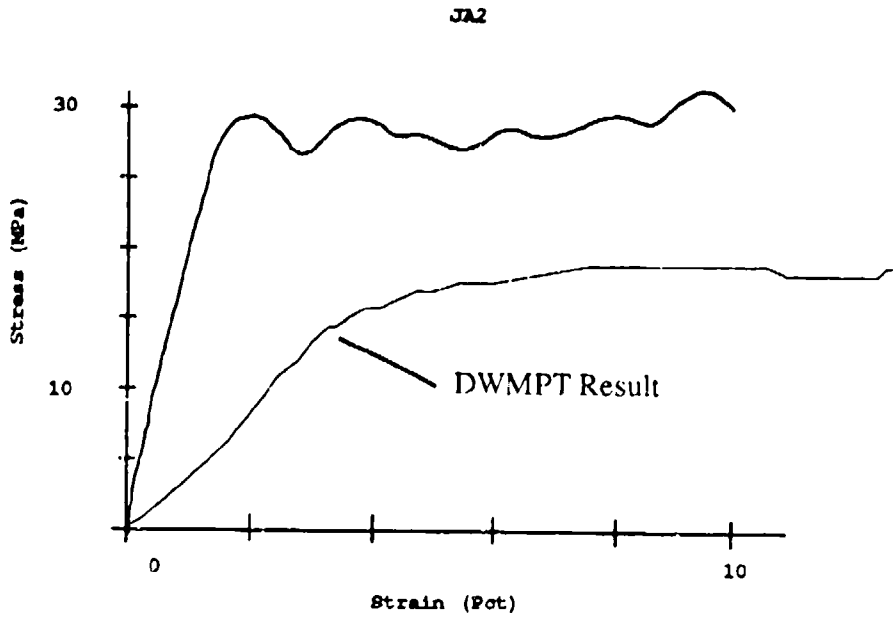

Figure 6b. Stress vs Strain

Figure 6. High Rate Response Curves for JA2 Seven-Multiperforated Propellant

Hopkinson
Split-Bar Test

ID = 1.136

L = 5.420 mm
D = 5.630 mm
XA = 24.30 mm
T = 24.00 C
P = .1000 MPa

YS = 88.93 MPa
3S = 88.01 MPa
5S = 91.60 MPa

SY = 1.645 Pct
SR = 2437 1/s

E = 7.080 GPa
EF = 0.299 MPa
T' = 0.974 MPa

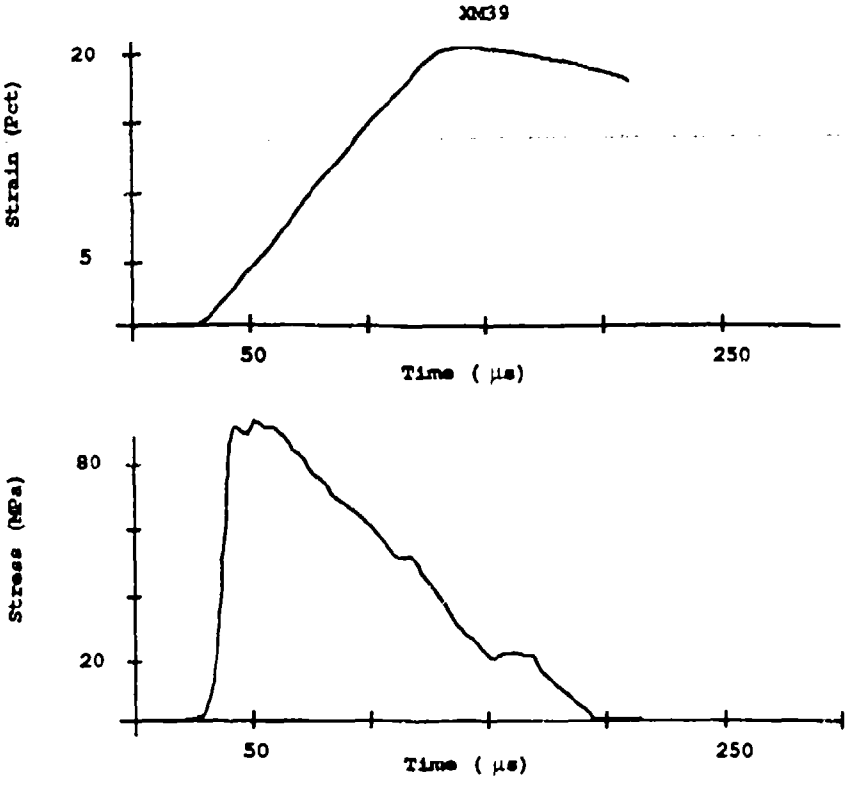

Figure 7a. Stress and Strain vs Time

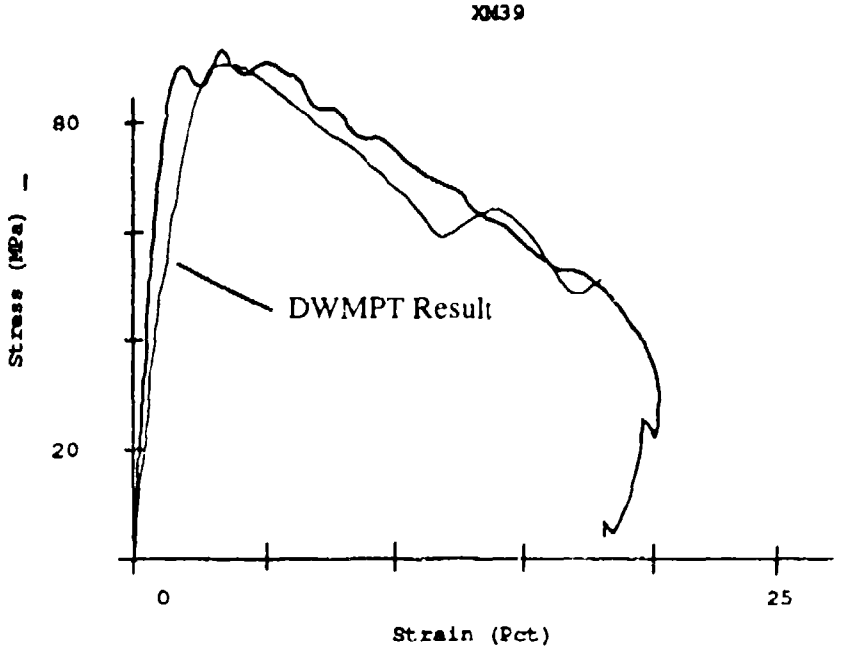

Figure 7b. Stress vs Strain

Figure 7. High Rate Response Curves for XM39 Seven-Multiperforated Propellant

Table 3. Comparison of Results From the Hopkinson Split Bar and Drop Weight Mechanical Properties Tests

Propellant		Strain Rate (1/s)	Yield Stress (MPa)	Yield Strain (%)	Modulus (GPa)
L/D = 1					
M30					
	HSB (STK)	1100	58.7	0.67	11.6
	HSB (7MP)	1620	68.9	1.50	5.4
	DWMPT*	247	81.0	3.94	3.0
JA2					
	HSB (7MP)	2070	29.7	1.67	2.25
	DWMPT	298	20.5	3.55	0.95
XM39					
	HSB (7MP)	2270	83.7	1.60	6.9
	DWMPT	346	82.0	3.21	3.9
L/D = 0.5					
	M30	2220	71.5	1.79	5.35
	JA2	3080	32.4	2.26	1.71
L/D < 0.5		(Individual Tests All 7MP)			
M30	L/D				
	0.338	6840	139	6.37	2.59
	0.201	11300	147	10.4	1.65
JA2	L/D				
	0.212	9450	50.0	7.11	0.835
	0.180	11080	47.5	4.25	1.29
XM39	L/D				
	0.372	7650	114	5.65	2.43

* All DWMPT Specimens are 7MP.

The significant differences noted above in the M30 response were originally thought to be the result of dewetting of the propellant binder (nitrocellulose) and crystal filler (nitroguanidine). Virgin and tested specimens were examined using a Scanning Electron Microscope for evidence of binder/filler separation. No indication of this was found, but even if this was known to occur, detection would be difficult. This is due to the SEM specimen preparation procedure, cold fracturing, which is required to observe the specimen interior. It could not be determined if the separation of

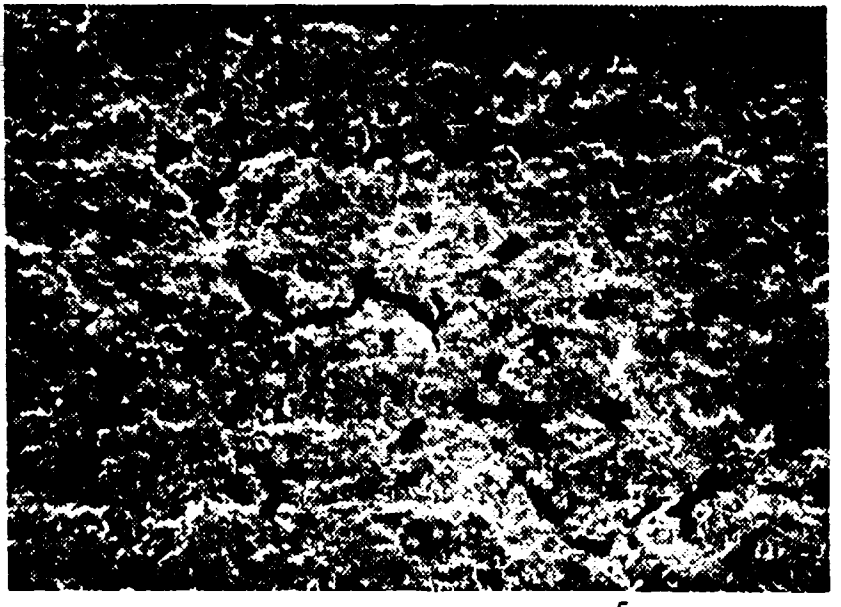

Figure 8. SEM Micrograph of the HSB Specimen End of Solid Stick M30 Showing Microporosity (1000X)

binder and filler was intrinsic to the specimen or an artifact of preparation. However, while observing the specimens with the SEM, intrinsic voids were observed on the ends of tested specimens. These voids, shown in Figure 8, were about 5 µm in diameter and a significant number were connected by cracks that ran through 5 to 20 of these voids. It is believed that the difference in response if the M30 is due, at least in part, to the presence of these and possibly other defects.

Multiperforated M30 was prepared and tested. A typical response curve along with a DWMPT curve is shown in Figure 9. This propellant is known to be free of voids and shows a response closer to what would be expected. The modulus is higher and even though yielding first occurs at a low stress, continued deformation showed no significant loss of strength. When significant yielding occurs at greater deformation, it occurs at stresses more in line with the expected values. The possibility of early separation of binder and filler still exists. However, the grossly deviant behavior observed in earlier tests has disappeared. The propellant had a higher modulus and appears to fail at a higher stress and lower strain, which was a shift toward more brittle behavior.

The response of specimens at L/D ratios less than 1 indicated that shear failure was occurring at lower strain. For these gun propellants it has been demonstrated that, for specimens with equal L/D ratios, as strain rate increases the yield stress, and modulus increase while the yield strain generally decreases. In these tests with L/D < 1, the stress and strain at yield increased, and the modulus decreased as L/D decreased in spite of the increase in strain rate. This was in conflict with previously observed results. The most likely explanation is a change of failure mode due to the L/D change.

Hopkinson
Split-Bar Test

ID = 1.224

L = 7.150 mm
D = 7.000 mm
XA = 35.70 mm²
T = 20.00 C
P = .1000 MPa

YS = 67.86 MPa
3S = 106.4 MPa
5S = 115.6 MPa

SY = 1.220 Pct
SR = 1696 1/s

E = 6.892 GPa
EF = -.145 MPa
T = 0.476 MPa

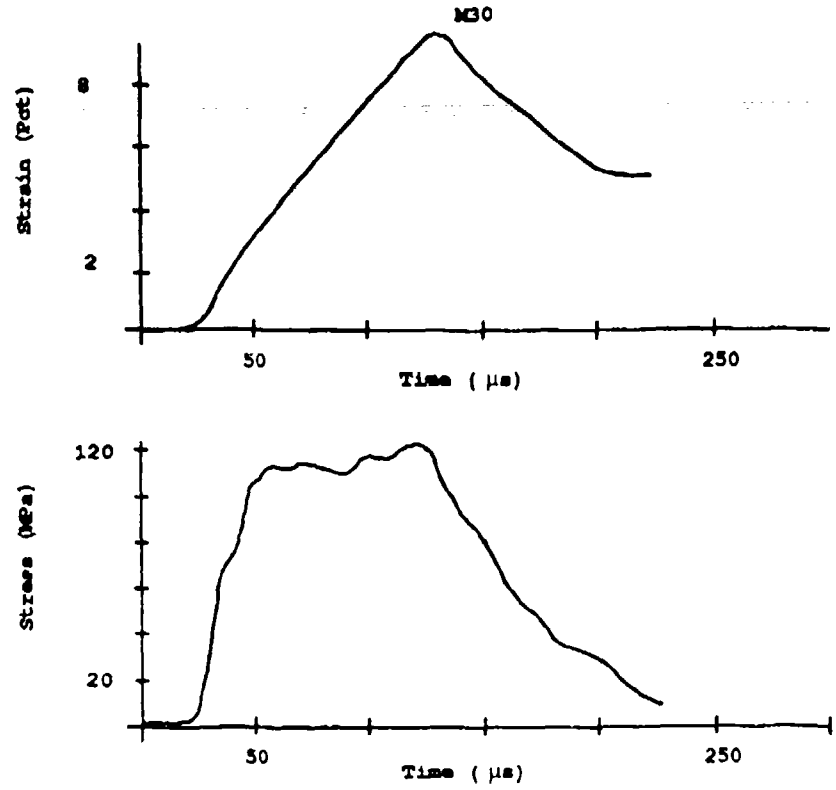

Figure 9a. Stress and Strain vs Time

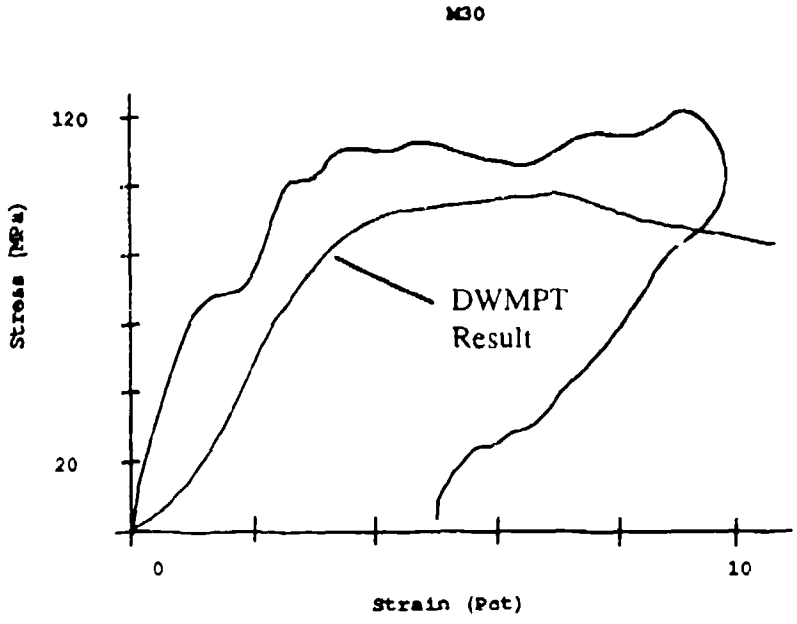

Figure 9b. Stress vs Strain

Figure 9. High Rate Response Curves for M30 Seven-Multiperforated Propellant

SEM micrographs were used to investigate the tested specimens. M30 and JA2 specimens with L/D > 0.3 remained intact with no visible fractures, and there was permanent deformation of about 20 percent. The XM39 specimens fractured into small shards. It is difficult to know when this occurred. The experiment ended as soon as the initial input pulse is fully reflected at the bar-specimen interface. Therefore it is not necessary for break-up of the specimen to be indicated by the signal although some fracture was indicated by the stress vs strain plots. The sample could be further damaged by reflected pulses as the bar moves after measurement is over. The thin specimens (L/D <0.3) suffered severe damage. JA2 specimens were in one piece, but were flattened with a 70 percent increase in diameter. There were also indications of brittle fracture, evidenced by cracks radiating from the perforations, as shown in Figure 10a. Most of the M30 specimens remained together, but they were badly fractured and had pieces missing. Micrographs, such as shown in Figure 10b, indicated much material flow as well as the occurrence of fracture. The XM39 specimens could not be found. Very small pieces of the specimen remained in the vicinity of the test site, and individual RDX Particles (5-10 μm) dusted the area. These particles were observed on micrographs of other specimens that were kept in the vicinity during the XM39 testing (see Figure 10a). All these observations are consistent with the measured results.

These results compare favorably with data generated at Lawrence Livermore National Laboratory[6,7] (LLNL). Figure 11 compares LLNL results with earlier DWMPT and the current HSB tests results. The LLNL specimens were of the same composition as the BRL specimens, but lot numbers and L/D ratios (LLNL used L/D ratio of 2) were different. However, the trends and magnitudes of the stress at 3-percent strain are comparable. Differences can be attributed to the specimen differences noted above. Figure 11b shows close agreement of the high rate modulus values for JA2, but the modulus obtained from the DWMPT data appears to be much lower than would be predicted by the LLNL data. However, another point of view can be taken. The lower rate LLNL data and the DWMPT data form a better fitting line than when all of the LLNL data is considered. The two highest modulus values are obtained by the same method (HSB). This may indicate that the measured modulus is influenced somewhat by the technique, or that a transition occurs somewhere above strain rates of about 300/s. The existence of this transition can be determined by lowering the impact velocity of the striker to obtain lower strain rates.

V. CONCLUSIONS

Hopkinson Split Bar data was collected and analyzed for three gun propellants, M30, JA2, and XM39. This device was constructed to extend the strain rate range of measurements beyond the 300/s limit currently available with the Drop Weight Mechanical Properties Test. Strain rates ranging from 1100 to 2270/s were obtained for specimens with a specimen length to diameter ratio of one. Test results indicated that at these higher rates yield stresses increased for M30 and JA2, but remained about the same for XM39. The initial moduli increased and the yield strains decreased for all propellants. The response at higher rates produced more fracture than tests at lower rates. However, the strength of the material before fracture appeared to increase with rate. These results agree with the results of similar tests conducted at Lawrence Livermore National Laboratory for JA2 and XM39 propellants.

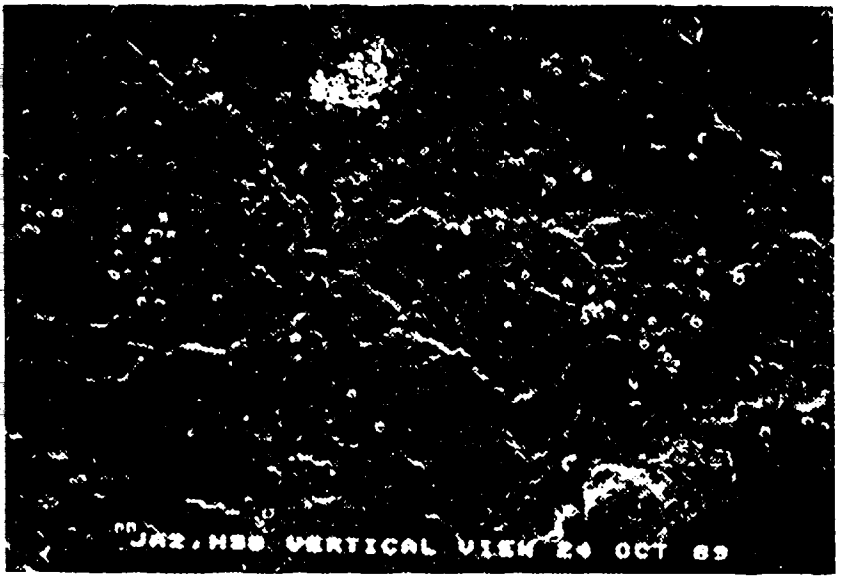

100 μm = ——

Figure 10a. JA2 Specimen Showing Fracture
(Perforation in the Lower Right Hand Corner, 50X)

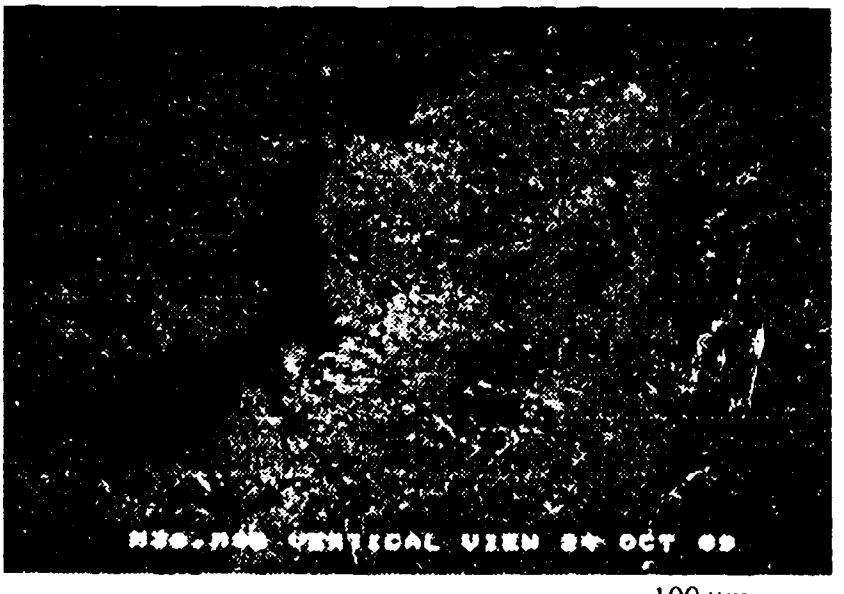

100 μm = ——

Figure 10b. M30 Specimen Showing Fracture and Plastic Flow (50X)

Figure 10. SEM Micrograph of Very Thin HSB Specimens

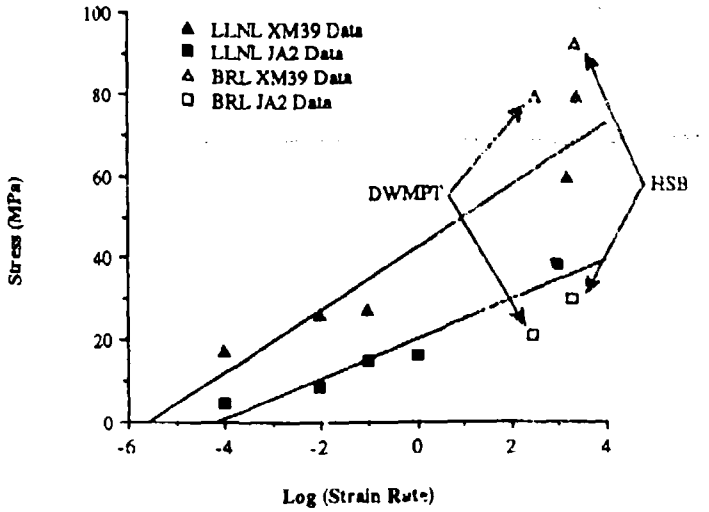

Figure 11a. Stress at 3-Percent Strain vs Log of Strain Rate

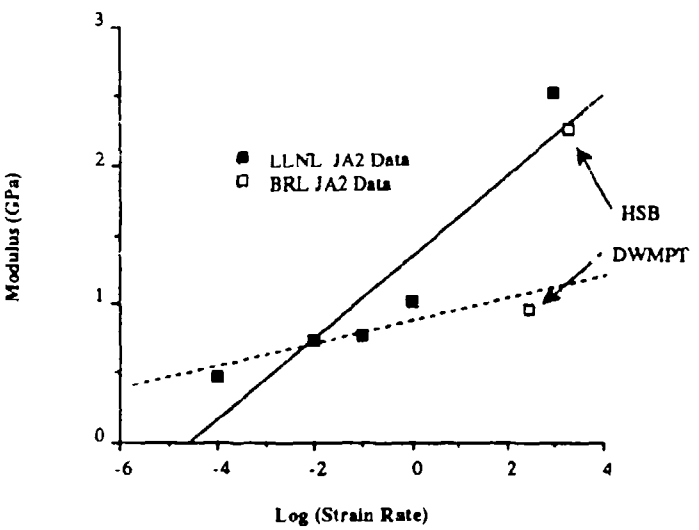

Figure 11b. Initial Modulus vs Log of Strain Rate

Figure 11. Comparison of BRL Results with LLNL Results (Solid Lines Represent the Best Fit to LLNL Data Points, the Dashed Line Represents the Best Fit to the Lower Rate Modulus Values)

Microporosity discovered in tested specimens appears to be responsible for the very high initial modulus values, the very low yield strain values, and the very weak response after yield obtained for M30 solid stick propellant. It was thought that the porosity precipitated local shear failure at low strain, which continued with deformation. Subsequent testing using specimens without voids provided a response more in line with other results. There was still some indication in these later tests that part of the weaker response could be due to binder-filler dewetting occurring within M30 at these rates, although no morphology differences were observed when micrographs of tested and untested specimens were compared. Further investigation is indicated.

Specimen length to diameter ratios were demonstrated to affect measured results. When the L/D ratio was reduced to increase the strain rate, rates of over 10,000/s were obtained. Results showed that the stress increased, as expected, but the strain at yield increased and the modulus decreased. The later two observations run contrary to trends observed with specimens of constant L/D ratios tested at various rates. It was concluded that the shortened specimens induce earlier shear failure which produced these results. The HSB results from LLNL, where the L/D ratio was 2, seem to indicate that this effect is not so pronounced when L/D is increased from 1 to 2. However, since different lots and specimen configurations were used (LLNL used only solid stick) the effect is not clearly demonstrated.

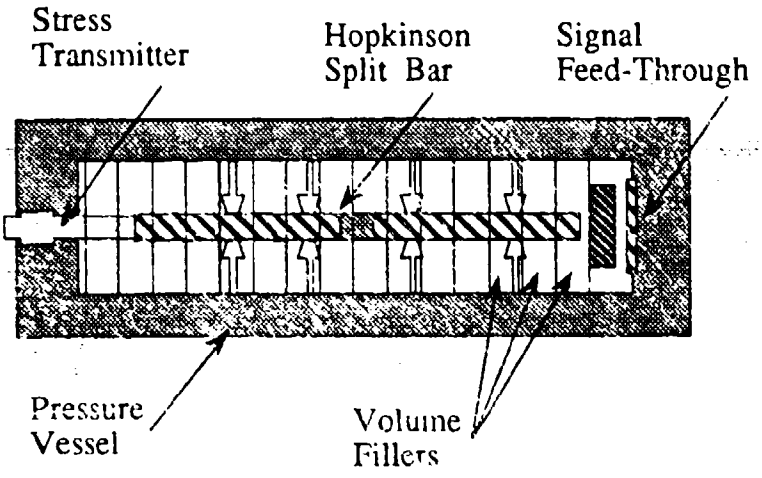

Figure 12. Schematic Diagram of the High Pressure Hopkinson Split Bar

VI. FUTURE EFFORTS

The Hopkinson Split Bar used here was designed to be part of a high pressure system that would permit high rate response measurements to be performed from ambient pressures up to 200 MPa. A schematic illustration of the assembled device is shown in Figure 12. The design and operation is fully explained in Reference 8, so only a brief explanation of the device will be provided here. The bar will be contained within a 1-inch smooth bore Mann barrel which is capped at both ends. One end contains an aluminium stress transmission bar which will deliver the stress pulse from the striker bar. The pulse is then transmitted into the high pressure confinement and delivered to the input bar. The experiment then proceeds as it does at atmospheric pressures. The signals from the strain gages, and other electronic information are sent by way of a special feed-through installed in the other cap that permits up to 16 signals to be delivered to the outside of the vessel. The pressurizing medium is gas, so volume fillers encircle the bar to reduce the free volume. The system is now ready to be pressure tested. When in operation, a large portion of the area indicated in Figure 1 as the "Critical Gun Regime" will be open for investigation. Plans are to conduct experiments on the propellants tested here in the near future, now that the HSB has been shown to provide satisfactory results.

REFERENCES

1. F. W. Robbins, Private Communication, BRL.

2. R. J. Lieb, "The Mechanical Response of M30, JA2 and XM39 Gun Propellants to High Rate Deformation," Technical Report (BRL-TR-3023) USA Ballistic Research Laboratory, Aberdeen Proving Ground, Maryland, August 1989.

3. R. J. Lieb, "Impact-Generated Surface Area in Gun Propellants," Technical Report (BRL-TR-2946, AD#-A200468), USA Ballistic Research Laboratory, Aberdeen Proving Ground, Maryland, November 1988.

4. R. J. Lieb, "High Rate Intrinsic Bed Response of Gun Propellant," 1987 JANNAF Structures & Mechanical Behavior Subcommittee Meeting, CPIA Publication 463, Volume I, pp 51-62, March 1987.

5. R. J. Lieb, D. Devynck, and J. J. Rocchio, "The Evaluation of High Rate Fracture Damage of Gun Propellant Grains," 1983 JANNAF Structure and Mechanical Behavior Subcommittee Meeting, CPIA Publication 388, pp 177-185, November 1983.

6. M. Costantino and D. Ornellas, "Initial Results for the Failure Strength of a LOVA Gun Propellant at high Pressures and Various Strain Rates," 1985 JANNAF Propulsion Meeting, CPIA Publication 425, pp 213-227, April 1985.

7. M. Costantino and D. Ornellas, "The High Pressure Failure Curve for JA2," 1987 JANNAF Structure and Mechanical Behavior Subcommittee Meeting, Volume I, CPIA Publication 463, pp 73-80, March 1987

8. H. J. Hoffman, " High-Strain Rate Testing of Gun Propellants," CPIA Publication 502, pp 51-61, December 1988.

9. H. Kolsky, "An Investigation of the Mechanical Properties of materials at Very High Rates of Loading," Proceedings of the Royal Society, Volume 62, p 676, 1949.

10. R. M. Davies, "A Critical Study of the Hopkinson Pressure Bar," Philosophical Transactions Acta., V 240, p 375, 1948.

11. F. E. Hauser, "Techniques for Measuring Stress-Strain Relations at High Rates," Experimental echanics, V 6, p 395, 1961.

12. "Wheatstone Bridge Nonlinearity," Measurements Group TECH NOTE, TN-507, Measurements Group, Inc., Raleigh, North Carolina, 1982.

13. U.S. Lindholm, "Some Experiments With The Split Hopkinson Pressure Bar," Journal of the Mechanics and Physics of Solids, V 12, pp 317-355, 1964.

Intentionally Left Blank

No of Copies	Organization
2	Administrator Defense Technical Info Center ATTN: DTIC-DDA Cameron Station Alexandria, VA 22304-6145
1	HQDA (SARD-TR) WASH DC 20310-0001
1	Commander US Army Materiel Command ATTN: AMCDRA-ST 5001 Eisenhower Avenue Alexandria, VA 22333-0001
1	Commander US Army Laboratory Command ATTN: AMSLC-DL Adelphi, MD 20783-1145
2	Commander US Army, ARDEC ATTN: SMCAR-IMI-I Picatinny Arsenal, NJ 07806-5000
2	Commander US Army, ARDEC ATTN: SMCAR-TDC Picatinny Arsenal, NJ 07806-5000
1	Director Benet Weapons Laboratory US Army, ARDEC ATTN: SMCAR-CCB-TL Watervliet, NY 12189-4050
1	Commander US Army Armament, Munitions and Chemical Command ATTN: SMCAR-ESP-L Rock Island, IL 61299-5000
1	Director US Army Aviation Research and Technology Activity ATTN: SAVRT-R (Library) M/S 219-3 Ames Research Center Moffett Field, CA 94035-1000

No of Copies	Organization
1	Commander US Army Missile Command ATTN: AMSMI-RD-CS-R (DOC) Redstone Arsenal, AL 35898-5010
1	Commander US Army Tank-Automotive Command ATTN: AMSTA-TSL (Technical Library) Warren, MI 48397-5000
1	Director US Army TRADOC Analysis Command ATTN: ATRC-WSR White Sands Missile Range, NM 88002-5502
(Class. only) 1	Commandant US Army Infantry School ATTN: ATSH-CD (Security Mgr.) Fort Benning, GA 31905-5660
(Unclass. only) 1	Commandant US Army Infantry School ATTN: ATSH-CD-CSO-OR Fort Benning, GA 31905-5660
1	Air Force Armament Laboratory ATTN: AFATL/DLODL Eglin AFB, FL 32542-5000
	Aberdeen Proving Ground
2	Dir, USAMSAA ATTN: AMXSY-D AMXSY-MP, H. Cohen
1	Cdr, USATECOM ATTN: AMSTE-TD
3	Cdr, CRDEC, AMCCOM ATTN: SMCCR-RSP-A SMCCR-MU SMCCR-MSI
1	Dir, VLAMO ATTN: AMSLC-VL-D

No. of Copies	Organization
1	HQDA (SARDA) WASH DC 20310-2500
1	Commander US Army TSARCOM 4300 Goodfellow Boulevard St. Louis, MO 63120-1702
1	Commander US Army Missile and Space Intelligence Center ATTN: AIAMS-YDL Redstone Arsenal, AL 35898-5500
1	Commander US Army Tank-Automotive Command ATTN: AMSTA-CG Warren, MI 48090
1	Commander US Army TRAC-Ft. Lee Defense Logistics Studies Fort Lee, VA 23801-6140
1	Commander USA Concepts Analysis Agency ATTN: D. Hardison 8120 Woodmont Avenue Bethesda, MD 20014-2797
10	Central Intelligence Agency Office of Central Reference Dissemination Branch Room GE-47 HQS Washington, DC 20505
1	US Army Ballistic Missile Defense Systems Command Advanced Technology Center P.O. Box 1500 Huntsville, AL 35807-3801
1	Chairman DoD Explosives Safety Board Room 856-C Hoffman Bldg. 1 2461 Eisenhower Avenue Alexandria, VA 22331-0600

No. of Copies	Organization
1	Commander US Army Materiel Command ATTN: AMCPM-GCM-WF 5001 Eisenhower Avenue Alexandria, VA 22333-5001
1	Commander US Army Material Command ATTN; AMCDE-DW 5001 Eisenhower Avenue Alexandria, VA 22333-5001
5	PEO-Armaments Project Manager Autonomous Precision-Guided Munition (APGM) US Army, ARDEC ATTN: AMCPM-CWA, H. Hassmann AMCPM-CWW AMCPM-CWW, F. Menke AMCPM-CWS, M. Fisette AMCPM-CWA-S, R. DeKleine Picatinny Arsenal, NJ 07806-5000
1	Project Manager Production Base Modernization Agency ATTN: AMSMC-PBM-E, L. Laibson Picatinny Arsenal, NJ 07806-5000
3	PEO-Armaments Project Manger Tank Main Armament Systems ATTN: AMCPM-TMA, K. Russell AMCPM-TMA-105 AMCPM-TMA-120 Picatinny Arsenal, NJ 07806-5000
8	Commander US Army, ARDEC ATTN: SMCAR-AEE-B, A. Beardell B. Brodman D. Downs S. Einstein S. Westley S. Bernstein C. Roller J. Rutkowski Picatinny Arsenal, NJ 07806-5000

No. of Copies	Organization
2	Commander US Army ARDEC ATTN: SMCAR-AES SMCAR-AES, D. Spring Picatinny Arsenal, NJ 07806-5000
3	Commander US Army, ARDEC ATTN: SMCAR-HFM, E. Barrieres R. Davitt SMCAR-CCH-V, C. Mandala Picatinny Arsenal, NJ 07806-5000
1	Commander US Army, ARDEC ATTN: SMCAR-FSA-T, M. Salsbury Picatinny Arsenal, NJ 07806-5000
1	Commander, USACECOM R&D Technical Library ATTN: ASQNC-ELC-I-T, Myer Center Fort Monmouth, NJ 07703-5301
1	Commander US Army Harry Diamond Laboratories ATTN: SLCHD-TA-L 2800 Powder Mill Rd Adelphi, MD 20783-1145
1	Commandant US Army Aviation School ATTN: Aviation Agency Fort Rucker, AL 36360
1	Project Manager US Army Tank-Automotive Command Improved TOW Vehicle ATTN: AMCPM-ITV Warren, MI 48397-5000
2	Program Manager US Army Tank-Automotive Command ATTN: AMCPM-ABMS, T. Dean Warren, MI 48092-2498
1	Project Manager US Army Tank-Automotive Command Fighting Vehicle Systems ATTN: AMCPM-BFVS Warren, MI 48092-2498
1	President US Army Armor and Engineer Board ATTN: ATZK-AD-S Fort Knox, KY 40121-5200
1	Project Manager US Army Tank-Automotive Command ATTN: AMCPM-ABMS Warren, MI 48092-2498
1	Director HQ, TRAC RPD ATTN: ATRC-MA, MAJ Williams Fort Monroe, VA 23651-5143
2	Director US Army Materials Technology Laboratory ATTN: SLCMT-ATL Watertown, MA 02172-0001
1	Commander US Army Research Office ATTN: Technical Library P. O. Box 12211 Research Triangle Park, NC 27709-2211
1	Commander US Army Belvoir Research and Development Center ATTN: STRBE-WC Fort Belvoir, VA 22060-5006
1	Director US Army TRAC-Ft Lee ATTN: ATRC-L, Mr. Cameron Fort Lee, VA 23801-6140
1	President US Army Artillery Board Ft. Sill, OK 73503-5000

No. of Copies	Organization
1	Commandant US Army Special Warfare School ATTN: Rev and Tng Lit Div Fort Bragg, NC 28307
3	Commander Radford Army Ammunition Plant ATTN: SMCAR-QA/HI LIB Radford, VA 24141-0298
1	Commander US Army Foreign Science and Technology Center ATTN: AMXST-MC-3 220 Seventh Street, NE Charlottesville, VA 22901-5396
2	Commander Naval Sea Systems Command ATTN: SEA 62R SEA 64 Washington, DC 20362-5101
1	Commander Naval Air Systems Command ATTN: AIR-954-Technical Library Washington, DC 20360
1	Assistant Secretary of the Navy (R, E, and S) ATTN: P Reichenbach Room 5[illegible]/ Pentagon Bldg Washington, DC 20375
1	Naval Research Laboratory Technical Library Washington, DC 20375
1	Commandant US Army Command and General Staff College Fort Leavenworth, KS 66027
2	Commandant US Army Field Artillery Center and School ATTN: ATSF-CO-MW, B. Willis Ft. Sill, OK 73503-5600

No. of Copies	Organization
1	Office of Naval Research ATTN: Code 473, R. S. Miller 800 N. Quincy Street Arlington, VA 22217-9999
3	Commandant US Army Armor School ATTN: ATZK-CD-MS, M. Falkovitch Armor Agency Fort Knox, KY 40121-5215
2	Commander US Naval Surface Warfare Center ATTN: J. P. Consaga C. Gotzmer Indian Head, MD 20640-5000
4	Commander Naval Surface Warfare Center ATTN: Code 240, S. Jacobs Code 730 Code R-13, K. Kim Code R-10, R. Bernecker Silver Spring, MD 20903-5000
2	Commanding Officer Naval Underwater Systems Center ATTN: Code 5B331, R. S. Lazar Technical Library Newport, RI 02840
5	Commander Naval Surface Warfare Center ATTN: Code G33, J. L. East W. Burrell J. Johndrow Code G23, D. McClure Code DX-21, Technical Library Dahlgren, VA 22448-5000
	Commander Naval Weapons Center ATTN: Code 388, C. F. Price Code 3895, T. Parr Information Science Division China Lake, CA 93555-6001

No. of Copies	Organization
5	Commander Naval Ordnance Station ATTN: L. Torreyson T. C. Smith D. Brooks W. Vienna Technical Library Indian Head, MD 20640-5000
1	AL/TSTL (Technical Library) ATTN: J. Lamb Edwards AFB, CA 93523-5000
1	AFATL/DLYV Eglin AFB, FL 32542-5000
1	AFATL/DLXP Eglin AFB, FL 32542-5000
1	AFATL/DLJE Eglin AFB, FL 32542-5000
1	NASA/Lyndon B. Johnson Space Center ATTN: NHS-22, Library Section Houston, TX 77054
1	AFELM, The Rand Corporation ATTN: Library D 1700 Main Street Santa Monica, CA 90401-3297
1	Hercules Incorporated ATTN: R. V. Cartwright Howard Boulevard Kenvil, NJ 07847
1	Scientific Research Assoc., Inc. ATTN: H. McDonald P.O. Box 498 Glastonbury, CT 06033-0498
1	United Technologies Corporation Chemical Systems Division ATTN: Tech Library P.O. Box 49028 San Jose, CA 95161-9028

No. of Copies	Organization
1	AAI Corporation ATTN: J. Frankle P. O. Box 126 Hunt Valley, MD 21030-0126
1	Aerojet General Corporation ATTN: D. Thatcher P.O. Box 296 Azusa, CA 91702
1	Aerojet Solid Propulsion Company ATTN: P. Micheli Sacramento, CA 96813
1	Atlantic Research Corporation ATTN: M. King 5390 Cherokee Avenue Alexandria, VA 22312-2302
3	AL/LSCF ATTN: J. Levine L. Quinn T. Edwards Edwards AFB, CA 93523-5000
1	AVCO Everett Research Laboratory ATTN: D. Stickler 2385 Revere Beach Parkway Everett, MA 02149-5936
2	Calspan Corporation ATTN: C. Murphy P. O. Box 400 Buffalo, NY 14225-0400
1	IITRI ATTN: M. J. Klein 10 W. 35th Street Chicago, IL 60616-3799
1	Hercules, Inc. Allegheny Ballistics Laboratory ATTN: William B. Walkup P. O. Box 210 Rocket Center, WV 26726

No. of Copies	Organization
1	Hercules, Inc. Radford Army Ammunition Plant ATTN: J. Pierce Radford, VA 24141-0299
3	Lawrence Livermore National Laboratory ATTN: L-355, A. Buckingham M. Finger L-324, M. Constantino P. O. Box 808 Livermore, CA 94550-0622
1	Olin Corporation Badger Army Ammunition Plant ATTN: F. E. Wolf Baraboo, WI 53913
1	Olin Corporation Smokeless Powder Operation ATTN: D. C. Mann P. O. Box 222 St. Marks, FL 32355-0222
1	Paul Gough Associates, Inc. ATTN: Dr. Paul S. Gough 1048 South Street Portsmouth, NH 03801
1	Physics International Company ATTN: Library, H. Wayne Wampler 2700 Merced Street San Leandro, CA 98457-5602
1	Princeton Combustion Research Laboratory, Inc. ATTN: M. Summerfield 475 US Highway One Monmouth Junction, NJ 08852-9650
2	Rockwell International Rocketdyne Division ATTN: BA08, J. E. Flanagan J. Gray 6633 Canoga Avenue Canoga Park, CA 91303-2703

No. of Copies	Organization
3	Thiokol Corporation Huntsville Division ATTN: D. Flanigan Dr. John Deur Technical Library Huntsville, AL 35807
2	Thiokol Corporation Elkton Division ATTN: R. Biddle Technical Library P. O. Box 241 Elkton, MD 21921-0241
1	Veritay Technology, Inc. ATTN: E. Fisher 4845 Millersport Highway East Amherst, NY 14501-0305
1	Universal Propulsion Company ATTN: H. J. McSpadden Black Canyon Stage 1 Box 1140 Phoenix, AZ 84029
1	Battelle Memorial Institute ATTN: Technical Library 505 King Avenue Columbus, OH 43201-2693
1	Brigham Young University Department of Chemical Engineering ATTN: M. Beckstead Provo, UT 84601
1	Vanderbilt University Mechanical Engineering ATTN: A. M. Mellor Box 6019, Station B Nashville, TN 37235
1	California Institute of Technology 204 Karman Laboratory Main Stop 301-46 ATTN: F.E.C. Culick 1201 E. California Street Pasadena, CA 91109

No. of Copies	Organization
1	California Institute of Technology Jet Propulsion Laboratory ATTN: L. D. Strand, MS 512/102 4800 Oak Grove Drive Pasadena, CA 91109-8099
1	University of Illinois Department of Mechanical/Industrial Engineering ATTN: H. Krier 144 MEB; 1206 N. Green Street Urbana, IL 61801-2978
1	University of Massachusetts Department of Mechanical Engineering ATTN: K. Jakus Amherst, MA 01002-0014
1	University of Minnesota Department of Mechanical Engineering ATTN: E. Fletcher Minneapolis, MN 55414-3368
3	Georgia Institute of Technology School of Aerospace Engineering ATTN: B.T. Zinn E. Price W.C. Strahle Atlanta, GA 30332
1	Institute of Gas Technology ATTN: D. Gidaspow 3424 S. State Street Chicago, IL 60616-3896
1	Johns Hopkins University Applied Physics Laboratory Chemical Propulsion Information Agency ATTN: T. Christian Johns Hopkins Road Laurel, MD 20707-0690
1	Massachusetts Institute of Technology Department of Mechanical Engineering ATTN: T. Toong 77 Massachusetts Avenue Cambridge, MA 02139-4307
1	Pennsylvania State University Applied Research Laboratory ATTN: G.M. Faeth University Park, PA 16802-7501
1	Pennsylvania State University Department of Mechanical Engineering ATTN: K. Kuo University Park, PA 16802-7501
1	Purdue University School of Mechanical Engineering ATTN: J. R. Osborn TSPC Chaffee Hall West Lafayette, IN 47907-1199
1	SRI International Propulsion Sciences Division ATTN: Technical Library 333 Ravenwood Avenue Menlo Park, CA 94025-3493
1	Rensselaer Ploytechnic Institute Department of Mathematics Troy, NY 12181
1	Stevens Institute of Technology Davidson Laboratory ATTN: R. McAlevy, III Castle Point Station Hoboken, NJ 07030-5907
1	Rutgers University Department of Mechanical and Aerospace Engineering ATTN: S. Temkin University Heights Campus New Brunswick, NJ 08903
1	University of Southern California Mechanical Engineering Department ATTN: OHE200, M. Gerstein Los Angeles, CA 90089-5199
2	University of Utah Department of Chemical Engineering ATTN: A. Baer G. Flandro Salt Lake City, UT 84112-1194

No. of
Copies Organization

1 Washington State University
Department of Mechanical Engineering
ATTN: C. T. Crowe
Pullman, WA 99163-5201

1 Alliant Techsystems, Inc.
ATTN: R. E. Tompkins
MN38-3300
10400 Yellow Circle Drive
Minnetonka, MN 55343

1 Science Applications, Inc.
ATTN: R. B. Edelman
23146 Cumorah Crest Drive
Woodland Hills, CA 91364-3710

Aberdeen Proving Ground

Dir, USAMSAA
ATTN: AMXSY-GI, CPT Klimack

USER EVALUATION SHEET/CHANGE OF ADDRESS

This Laboratory undertakes a continuing effort to improve the quality of the reports it publishes. Your comments/answers to the items/questions below will aid us in our efforts.

1. BRL Report Number BRL-TR-3200 Date of Report February 1991

2. Date Report Received _____

3. Does this report satisfy a need? (Comment on purpose, related project, or other area of interest for which the report will be used.) _____

4. Specifically, how is the report being used? (Information source, design data, procedure, source of ideas, etc.) _____

5. Has the information in this report led to any quantitative savings as far as man-hours or dollars saved, operating costs avoided, or efficiencies achieved, etc? If so, please elaborate. _____

6. General Comments. What do you think should be changed to improve future reports? (Indicate changes to organization, technical content, format, etc.) _____

CURRENT ADDRESS

Name

Organization

Address

City, State, Zip Code

7. If indicating a Change of Address or Address Correction, please provide the New or Correct Address in Block 6 above and the Old or Incorrect address below.

OLD ADDRESS

Name

Organization

Address

City, State, Zip Code

(Remove this sheet, fold as indicated, staple or tape closed, and mail.)

FOLD HERE

DEPARTMENT OF THE ARMY
Director
U.S. Army Ballistic Research Laboratory
ATTN: SLCBR-DD-T
Aberdeen Proving Ground, MD 21005-5066
OFFICIAL BUSINESS

NO POSTAGE NECESSARY IF MAILED IN THE UNITED STATES

BUSINESS REPLY MAIL
FIRST CLASS PERMIT No 0001, APG, MD

POSTAGE WILL BE PAID BY ADDRESSEE

Director
U.S. Army Ballistic Research Laboratory
ATTN: SLCBR-DD-T
Aberdeen Proving Ground, MD 21005-9989

FOLD HERE